Green synthesis of silver nanoparticles reduced with *Trigonella foenum-graecum* and their effect on tumor necrosis factor-α in MCF7 cells

A.A.H. ABDELLATIF[1,2], S.K. OSMAN[2], M. ALSHARIDAH[3], O. AL RUGAIE[4], T.M. FARIS[5], A. ALQASOUMI[6], A.M. MOUSA[7,8], A. BOUAZZAOUI[9,10,11]

[1]Department of Pharmaceutics, College of Pharmacy, Qassim University, Buraydah, Kingdom of Saudi Arabia
[2]Department of Pharmaceutics and Pharmaceutical Technology, Faculty of Pharmacy, Al-Azhar University, Assiut, Egypt
[3]Department of Physiology, College of Medicine, Qassim University, Buraydah, Saudi Arabia
[4]Department of Basic Medical Sciences, College of Medicine and Medical Sciences, Qassim University, Unaizah, Al Qassim, Saudi Arabia
[5]Department of Pharmaceutics and Industrial Pharmacy, College of Pharmacy, Al-Azhar University, Cairo, Egypt
[6]Department of Pharmacy Practice, College of Pharmacy, Qassim University, Qassim, Saudi Arabia
[7]Department of Basic Health Sciences, College of Applied Medical Sciences, Qassim University, Qassim, Saudi Arabia
[8]Department of Histology and Cell Biology, Faculty of Medicine, Benha University, Benha, Egypt
[9]Department of Medical Genetics, Faculty of Medicine, Umm Al-Qura University, Makkah, Saudi Arabia
[10]Science and Technology Unit, Umm Al-Qura University, Makkah, Saudi Arabia
[11]Medical Clinic, Hematology/Oncology, University Hospital Regensburg, Regensburg, Germany

Abstract. – **OBJECTIVE**: Silver nanoparticles (AgNPs) are known to exhibit anti-inflammatory and anticancer activities. They have been reported to reduce the levels of tumor necrosis factor (TNF) – a proinflammatory cytokine involved in cell proliferation, differentiation, and apoptosis – in cell lines. As patients with breast cancer have been reported to have higher serum TNF levels, we aimed at developing a novel treatment for breast cancer by evaluating the effect of *Trigonella foenum-graecum* extract (TFG)-reduced AgNPs on the MCF-7 cell line, which serves as a model of human breast cancer.

MATERIALS AND METHODS: TFG-capped AgNPs were synthesized using a green reduction method, in which TFG reduced silver nitrate to generate AgNPs-TFG. The particle size, surface charge, ultraviolet (UV)-visible (VIS) spectra, surface morphology, % yield, and *in vitro* Ag+ release of the formulated AgNPs-TFG were evaluated. Additionally, the prepared NPs were examined for cytotoxicity using real-time polymerase chain reaction (real-time PCR), 3-(4,5-dimethylthiazol-2-yl)-2,5-diphenyltetrazolium bromide (MTT) assay, and enzyme-linked immunosorbent assay (ELISA).

RESULTS: The prepared AgNPs-TFG were uniform, small, discrete, and non-aggregated with a particle size of 22.5±0.75 nm and ζ-potential of -47.45±0.666 mV. The yield of AgNPs-TFG was 224.545±3.9 μM. Furthermore, the AgNP-TFG thin film exhibited a prolonged release of Ag+ in phosphate buffer for up to 11 h. AgNPs-TFG suppressed TNF-α expression at mRNA and protein levels in MCF-7 cells. Additionally, the formulated AgNPs-TFG did not exhibit any toxicity toward MCF-7 cells.

CONCLUSIONS: This study showed that AgNP-TFG could effectively inhibit TNF-α. These results provide significant insights for developing new therapeutic strategies for cancer and other inflammatory illnesses.

Key Words:
   Silver nanoparticles, Tumor necrosis factor-α, MCF-7 cells, *Trigonella foenum-graecum*.

Introduction

Nanoparticles (NPs) have various applications and can enhance active and passive targeting. Silver NPs (AgNPs) can overcome the limitations associated with conventional NPs by employing passive targeting once the tumor has been located[1]. AgNPs exhibit effective antitumor activity because they target

Corresponding Authors: Ahmed A. H. Abdellatif, MD; e-mail: a.abdellatif@qu.edu.sa
Abdellatif Bouazzaoui, MD; e-mail: alazzauoi@uqu.edu.sa

specific types of cells. Furthermore, these NPs can penetrate solid tumors and eliminate distinct groups of cells that drive tumor growth. AgNPs function by absorbing photons, a phenomenon that generates heat that kills cancer cells[2]. Green NP synthesis makes the use of plant materials that are safer for the environment. Currently, the active compounds present in plants are used for imparting therapeutic properties to NPs in green synthesis. The medicinal plant fenugreek (*Trigonella foenum-graecum L. –* TFG) has been extensively used in tumor therapy, and is known to exhibit anticancer, antioxidant, antidiabetic, and antibacterial effects[3]. Furthermore, as they are generated in a single step, NPs synthesized using green technology have several advantageous properties, including increased stability and acceptable diameters[4].

Tumor necrosis factor-alpha (TNF-α) has been demonstrated to induce hemorrhagic necrosis in many cancers by interacting with specific cytokine receptors (TNFRs) expressed on the surface of cells lining the vascular endothelium[5]. TNF-α is associated with numerous activities, such as causing fever, apoptotic cell death, autonomic dysfunction and inflammation, and prevention of cancer[6,7]. Patients with breast cancer have been reported[8] to have higher levels of TNF-α in their plasma. Moreover, TNF-α has been reported[9] to be closely associated with NF-kβ-related genes in human breast cancer.

As nanomaterials trigger cytokine signaling, *in vitro* studies[10] have focused on the anti-inflammatory effects of AgNPs and their function in wound healing. Moreover, the antibacterial effects of AgNPs with respect to destruction of the bacterial wall have also been studied. We have previously reported[11,12] that AgNPs prepared using the citrate reduction method and ethyl cellulose reduction method have an anti-apoptotic effect and reduce the TNF-α levels in cell lines. TNF-α has been reported to induce apoptosis by releasing reactive oxygen species and activating caspases. AgNPs-TFG have been reported to inhibit TNF-α-induced apoptosis in MCF-7 cells[10].

In this study, we aimed at synthesizing AgNPs-TFG and examine their effect on TNF-α-induced apoptosis in MCF-7 cells. We hypothesized that AgNPs-TFG have anti-apoptotic and anti-inflammatory effects in breast cancer. To the best of our knowledge, no effort has been made to generate AgNP-TFG *via* facile green synthesis. We sought to produce colloidal AgNPs, using inexpensive materials and a facile and straightforward fabrication method. Our results revealed that the formulated green AgNPs could decrease the TNF-α levels in MCF7 cells. Thus, our approach could serve as a new strategy for treating cancer. Such procedures for producing green AgNPs would enable the commercialization of anticancer treatments at competitive costs. Therefore, this study was conducted to synthesize and characterize AgNPs using the aqueous extract of TFG seeds and investigate the effect of these green AgNPs on apoptosis, one of the most critical cellular responses.

Materials and Methods

Materials

Hydrogen tetrachloroaurate trihydrate was purchased from Sigma-Aldrich (Steinheim, Germany). *Trigonella foenum-graecum* L. seeds were purchased from a Saudi market (Buraidah, Qassim, KSA). Sodium chloride, sodium hydroxide, nitric acid, hydrochloric acid, triethylamine, sodium dihydrogen phosphate, disodium hydrogen phosphate, ethylenediaminetetraacetic acid, dimethylformamide, ethanol (100%), isopropanol, and chloroform were purchased from Merck (Darmstadt, Germany). 2,2-diphenyl-1-picrylhydrazyl (DPPH) was purchased from Sigma-Aldrich (St. Louis, MO, USA). Iscove's Modified Dulbecco's medium was purchased from Invitrogen (Carlsbad, CA, USA), and iron-supplemented calf serum was obtained from HyClone Laboratories (Logan, UT, USA). Antibodies were purchased from Cell Signaling Technology Inc. (Danvers, MA, USA) and Santa Cruz Biotechnology, Inc. (Santa Cruz, CA, USA). The kits for performing cytokine-specific enzyme-linked immunosorbent assays (ELISAs) were purchased from R&D Systems (St. Paul, MN, USA). A kit for assaying the IKK activity was purchased from Cell Signaling Technology Inc. MCF-7 cells were obtained from the ATCC (Manassas, VA, USA). All chemicals were of analytical grade. All glassware was washed with distilled water and dried in an oven at 40°C.

Preparation and Characterization of AgNPs-TFG

Preparation of AgNPs-TFG
Colloidal AgNPs-TFG were produced via green reduction[3]. The seeds were washed and steeped for one hour to remove the outermost layer of dust. The seeds were rinsed a second

time and cooked in 100 mL sterile distilled water for 30 min. The mixture was then centrifuged at 1000 rpm for 15 min in an Optima™ Max-E Ultra Cooling Centrifuge (Beckman Coulter, Pasadena, CA, USA), and the supernatant was collected. The supernatant was placed in a brown bottle and stored in the dark for 24 h. Following incubation, the supernatant was mixed with fresh 1 mM silver nitrate and incubated with continuous stirring at 600 rpm for 12 h. During incubation, the color of the solution changed from yellow to red, indicating the formation of AgNPs. Drying and centrifugation were performed to remove contaminants; all these procedures made the fluid an effective nutrient solution.

Size and zeta potential determination

The size, polydispersity index (PDI), and zeta potential (ζ-potential) of the obtained Ag-NPs-TFGs were evaluated using a Zetasizer Nano ZS (Malvern Instruments GmbH, Herrenberg, Germany). The samples were pre-equilibrated at 25°C, and each sample was exposed to a laser beam (633 nm) at a scattering angle of 90°. Three measurements were conducted for each sample, and each reading was the mean of ten internal sub-runs of the Nano ZS. The backscattering was 173°, and the measurement location was set at 4.65 mm. The duration between each run was 60 s with equilibration of 180 s. The measurements were conducted in water. The readings were averaged, and each measure was tested 20 times (which equated to 10 s)[11-15].

UV-VIS spectroscopy

The absorbance spectra of AgNPs-TFG were measured using a Uvikon 941 UV-VIS spectrophotometer (Kontron Instruments GmbH, Tokyo, Japan)[11,12,15].

Scanning electron microscopy

AgNPs (~20 µL) were placed on the surface of a double-sided copper conductive tape and allowed to dry. The NPs were then sputter-coated (JOEL JFC-1300, Augsburg, Germany) with a thin layer of platinum in a vacuum chamber for 1 min at 25 Å to make them electrically conductive before imaging. Scanning electron microscopy (SEM) was used to examine the shape and size of the produced AgNPs (JEOL JSM-550, Tokyo, Japan)[16].

AgNP percentage yield

The amount of Ag^+ converted into Ag^0 was calculated using a previously described approach

with some minor modifications[15,17]. The produced AgNPs-TFG were centrifuged at 2000 rpm for 5 min to separate the large particulates and remove impurities. The supernatant was evaluated using inductively coupled plasma optical emission spectrometry (ICP-OES; iCAP 6000, Thermo Scientific, Washington, USA) to calculate the amount of Ag^0 in the AgNPs. Each solution was scanned five times. The percentage yield of the produced AgNPs was calculated by dividing the obtained concentration of Ag^0 by the initial concentration of $AgNO_3$, and then multiplying the same per 100 (Eq. 1).

$$\% \, AgNP \, Yield = \left[\frac{Concentration \, of \, each \, sample \, by \, ICP \, OES}{Initial \, Concentration \, of \, AgNP3} \right] \times 100 \quad Eq. 1$$

Silver ion release

Silver ions were released by the formulated AgNPs-TFG[18]. Thin films of AgNPs-TFG were produced using roughly 2.0 cm^2 of the AgNPs-TFG and incubated in 50 mL deionized water for 24 h at 25°C. After rigorous calibration with the reference silver solution, samples were obtained at various time points to measure silver cation utilization (ICP-OES). The experiment was conducted in triplicate at room temperature (25°C) in a shaking incubator (WiseShak, SHO-2D, Korea), rotating at 100 rpm.

Cell Culture

MCF-7 cells were obtained from the American Type Culture Collection (ATCC, Manassas, VA, USA) and were cultured in RPMI-1640 medium supplemented with 10% heat-inactivated fetal bovine serum (FBS) and 1% penicillin-streptomycin at 37°C in an atmosphere containing 5% CO_2. MCF-7 cells that were not treated with AgNP-TFG served as the negative control, and MCF-7 cells treated with $AgNO_3$ served as a positive control[11,12].

Treatment of MCF-7 Cells with AgNPs-TFG

MCF-7 cells (1×10^6 cells/mL) were seeded in 35-mm culture plates (Becton-Dickinson, Franklin Lakes, NJ, USA) and serum-starved for 24 h in RPMI medium. Following which, the cells were treated with various concentrations of AgNPs-TFG for 24 h, after which cytotoxicity was assessed using the CytoTox-GloTM Cytotoxicity Assay Kit (Promega, Madison, WI, USA), as previously described[19]. Cells treated with $AgNO_3$ (0.1-200 µM) served as a positive control. In other sets of experiments, MFC-7 cells were treated for 48 h with 200 µM AgNPs-TFG[11,12].

Quantitative Real-Time PCR

As previously stated, real-time quantitative PCR was used to evaluate the expression of TNF-α, with GAPDH serving as an internal control[11,12]. In accordance with the manufacturer's instructions, total RNA was isolated using the mirVana RNA isolation kit (catalog #AM1560; Ambion Inc., Foster City, CA, USA). One to two milligrams of total RNA were reverse-transcribed into cDNA using a SuperScript First Strand cDNA Synthesis Kit (Catalog #4368814, Applied Biosystems, Foster City, CA, USA). TaqMan gene expression arrays (Applied Biosystems) were used to measure the amount of TNF mRNA in the blood. The Step One Real-Time PCR System was used for real-time PCR and data collection (Applied Biosystems). The following primers were used for PCR amplification: IL-1 beta (NM 000595): forward, 5'-AGG ACG AAC ATC CAA CCT CAA-3'; reverse, 5'-TTTGAGCCAGAAGGGGGGGGT-3' and GAPDH (NM 002046.3): forward, 5'-AC-CAAATCCGTTGACCTTGACCTT-3'). Melt curve analysis was performed using the following cycle: 96°C for 10 min, followed by 40 cycles of 96°C for 15 s and 64°C for 65 s. The expression of target mRNA was normalized to that of GAPDH and then compared with its expression level in the untreated sample[20].

TNF-α ELISA

MCF-7 cells were pretreated with various concentrations of AgNPs-TFG (1-200 μM). TNF-α levels in the culture media were measured using a TNFα-specific ELISA kit (R&D Systems, Minneapolis, MN, USA). Absorbance was read using an automated microplate reader (Anthos Zenyth 3100 Multimode Detectors, Salzburg, Austria), in accordance with the protocol provided along with the ELISA kit[11].

Statistical Analysis

Data are expressed as means of at least three experiments with standard deviations. The SPSS software was used to perform one- or two-sample t-tests (IBM, Armonk, NY, USA). *$p<0.05$, **$p<0.01$, or ***$p<0.001$ was considered statistically significant.

Results

Synthesis of AgNPs-TFG

AgNPs-TFG were synthesized using the one-step reduction approach. A color change was observed when the TFG extracted from sees was mixed with AgNO$_3$. The reaction medium showed a yellow color that turned crimson after complete synthesis. The produced NPs were characterized for particle size (hydrodynamic diameter), PDI, and charge[21,22]. Our results revealed that the AgNPs-TFG were tiny and homogenous in size (22.5±0.75 nm) (Figure 1A). Furthermore, the mean count rate was recorded as (188 kpcs), which is high enough, indicating that the concentration of AgNPs-TFG was sufficient for the measurements to be made. Figure 1B shows that the AgNPs-TFG had a significant negative surface charge (-47.40.666 mV), also the PDI was relatively modest and accepted which recorded (0.16).

The UV-VIS spectra of the AgNPs-TFG revealed a surface plasmon resonance peak at 386.6 nm, corresponding to the material's highest absorbance (Figure 2A). The AgNP formulations were often detected as small discrete entities, either singly or as clustered lumps of NPs with regular or irregular shapes (Figure 2B). Moreover, AgNPs. TFG were highly spotted NPs with more uniform and non-aggregated particles (Figure 2B), confirming the findings of the dynamic light scattering investigation[23].

The Percent Yield of Synthesized AgNPs

Table I shows the initial Ag$^+$ and Ag^0 concentrations in the AgNPs following NP formation, as measured by ICP-OES. The percent yield was calculated for Ag^0 synthesized in the AgNPs-TFG at 224.57±3.9 μM (41.28%).

Silver Ion Release

Figure 3 shows the release of Ag^0 from the synthesized AgNPs-TFG in deionized water. Ag^0 was released continually in aqueous solutions for approximately 11 h; it was slowly released from AgNPs-TFG owing to the weak solubility of TFG in water[24,25].

Effects of AgNPs in MCF-7 Breast Cancer Cells

MCF-7 cells were treated with AgNPs-TFG or AgNO$_3$ at concentrations of 0.1-200 μM for 24 h (Figure 4). After 24 h, MCF-7 cells were examined using MTT assays to determine cytotoxicity. Various incubation times, i.e., 6-48 h were used in the presence of 200 μM AgNPs-TFG. MTT assays demonstrated that the formulated AgNPs-TFG were not cytotoxic compared with the starting material AgNO$_3$; the control showed higher toxicity toward MCF-7
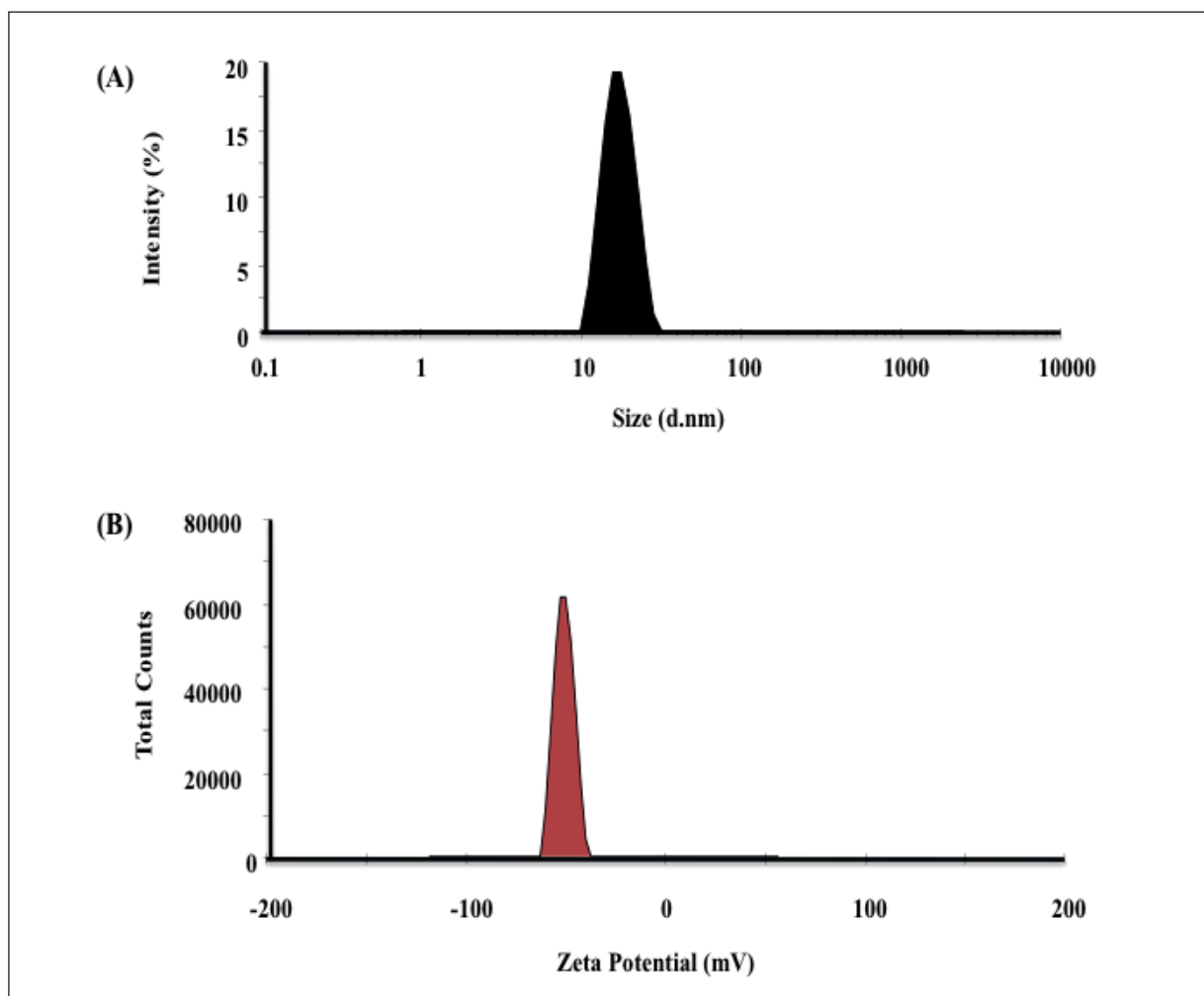
Figure 1. Particle size distribution and ζ-potential measurements of AgNPs-TFG. **A,** Particle size distribution of AgNPs-TFG. **B,** ζ-Potential of AgNPs-TFG having a negative surface charge. Each measure was the average of three trials.

cells. However, MCF-7 cells showed a reduced viability of 72.0%±3.66% compared to that of the untreated control when the concentration increased to 200 µM. Moreover, the Ag-NPs-TFG did not result in any marked reduction in the percent viability. The results showed a reduction of only 94.1%±2.66% compared to that of the untreated control when treated with a high concentration of 200 µM AgNPs-TFG (Figure 4).

In differentiated MCF-7 cells treated with AgNO₃ or AgNPs-TFG, cell proliferation was blocked by AgNO₃ and AgNPs-TFG. AgNO₃ showed greater inhibitory effects than Ag-NPs-TFG. As MCF-7 cells differentiated further, cells showed non-significant reductions in the percent viability as the incubation time increased following treatment with AgNPs-TFG (Figure

5). By contrast, when MCF-7 cells were treated with AgNO₃ for 48 h, the degree of proliferation was significantly reduced to 63.1% compared to that of AgNPs-TFG-treated cells, which showed a reduction to only 92.1% that of the untreated control.

Next, we evaluated the effects of different concentrations of AgNPs-TFG (1-200 µM) on gene expression in MCF-7 cells. Our results showed that the synthesized AgNPs-TFG stimulated the cells and cause a considerable reduction in TNF-α mRNA levels. ELISA of cell supernatants showed that the AgNPs-TFG significantly reduced TNF-α levels when used at concentrations of 5-100 µM (Figure 6A and B, $p<0.05$). Maximum reduction was detected in cells treated with 100 µM AgNPs-TFG ($p<0.01$), after which no further significant decrease was observed un-
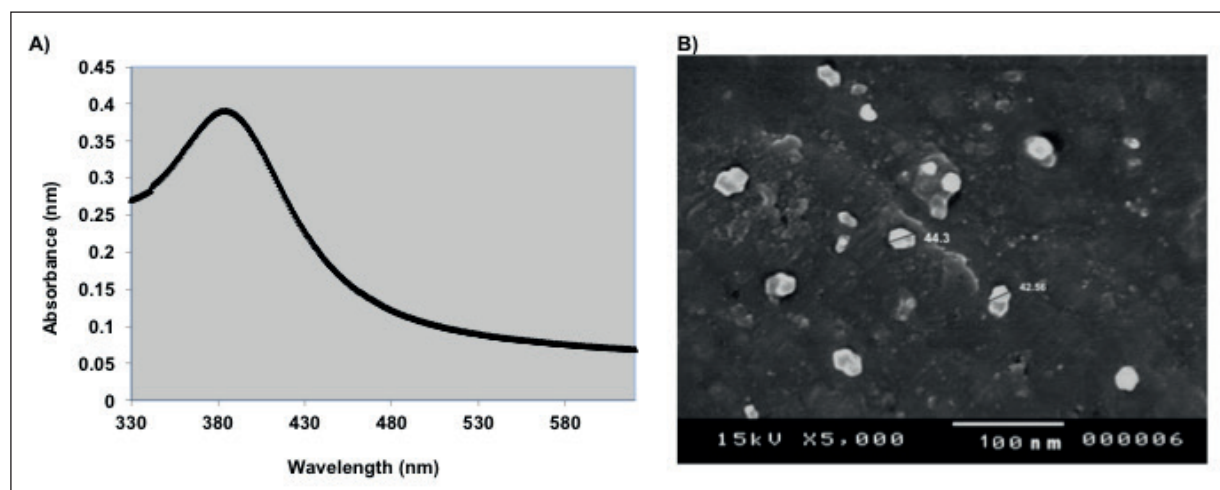
5533

Figure 2. A, UV-VIS spectra of AgNPs-TFG. AgNPs-TFG showed the maximum absorbance at 386.6 nm, consistent with the surface plasmon resonance peak. **B**, SEM image of AgNPs-TFG.

til the concentration reached 200 µM (Figure 6A and B).

Discussion

The prepared AgNPs-TFG were homogenous in size (22.5±0.75 nm) and showed a significant negative surface charge (-47.40.666 mV), indicating that the AgNPs-TFG were electrically stabilized and could resist particle aggregation[26]. The PDI was relatively modest (0.16), indicating that the colloidal AgNPs-TFG were well-controlled and standardized. It has been reported that PDI may be used to assess stability. Generally, a PDI <0.2 is considered ideal, as this value indicates that the particle size distribution falls within a narrow range. The surface charge of the NPs also plays a significant role in determining NP stability, and the magnitude of the potential indicates that the structure has been colloidally stabilized[27]. Interestingly, the results confirmed that the AgNPs-TFG were identical to those obtained in our previous work, ensuring the production and nucleation of TFG around the Ag[+11,12,15]. The significant interactions of Ag^{+} with TFG were verified in a coated layer. The AgNPs-TFG contained homogenous AgNPs, consistent with the findings of He et al[28]. Such interactions would reduce metallic cation mobility, inhibit the formation of large particles, and stabilize the synthesized AgNPs[23].

However, the percent yield did not reach 100% with the current synthesis method, although an acceptable percent yield was obtained for AgNPs-TFG. Inconsistencies between the reported and theoretical Ag inputs can also be ascribed to Ag^{+} or AgNP adsorption on the centrifuge tubes or pipets, volume loss, and sample loss during transfer for dilution and quantification procedures[17].

Ag[0] was released continually and slowly from AgNPs-TFG owing to the weak solubility of TFG in water. In previous studies[24,25], continual release of Ag[0] has been observed depending on the degree of solubility of TFG in water. Thus, the slow release of Ag[0] from AgNPs-TFG can be explained in terms of the film's coating shielding action, which reduces the water solubility of NPs. As a result, particle corrosion is first controlled by coating diffusion into the water,

Table I. The percent yield of Ag[0] in AgNPs after conversion of Ag^{+} to Ag[0].

	Concentration (µM)	% yield (Conversion %)
AgNPs-TFG	224.57±3.9	41.28±7.6
Ag^{+} (initial concentration)	54 ±0.5	--------

Notes: Each solution was scanned five times. The % yield of the produced AgNPs was calculated by dividing the obtained Ag[0] concentration in the supernatant by the initial concentration of AgNO$_3$.
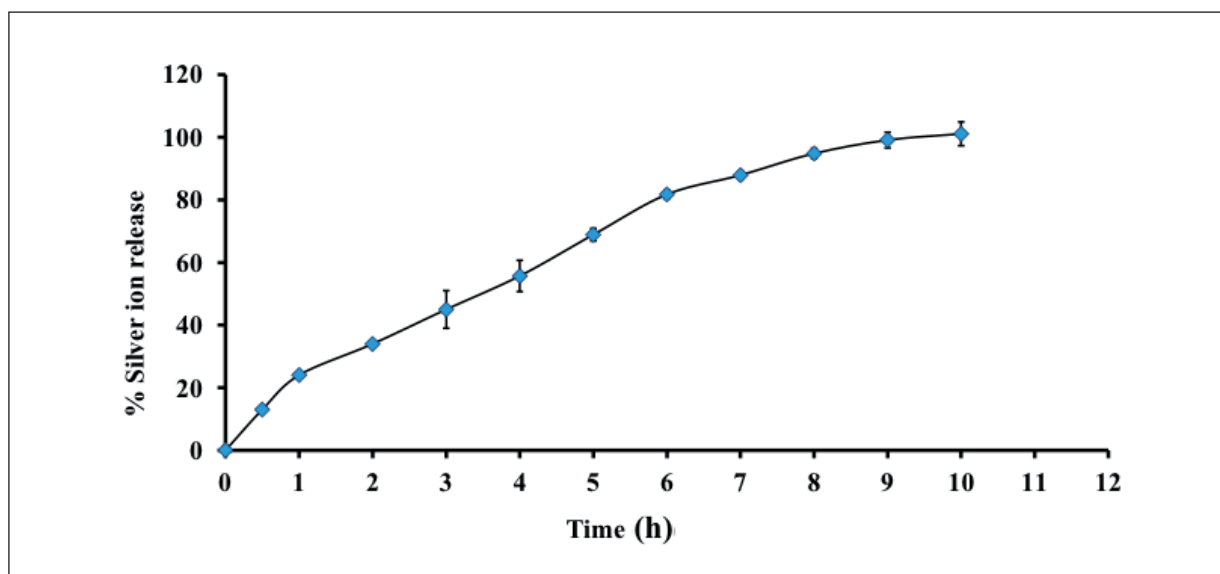
Figure 3. *In vitro* Ag^0 release from the prepared AgNPs-TFG in deionized water (n=3; means±standard deviations).

which slows cation release. The depletion of the coating surrounding the AgNPs then enhances the rate of Ag^0 release, in accordance with ICP-OES observations[18].

MTT assays demonstrated that AgNPs-TFG were not cytotoxic, compared with the starting material $AgNO_3$ which showed higher toxicity toward MCF-7 cells. The cytotoxic and harmful effects of $AgNO_3$ have been demonstrated *in vitro* in rat hepatocytes[29], human lymphocytes[30], and keratinocytes[31]. Furthermore, $AgNO_3$ has antimicrobial and anticancer effects, and silver has been shown to be cytotoxic at both low and high doses[32]. Notably, silver compounds have exhibited anticancer properties and inhibitory effects in the context of L9291 immortalized murine fibroblasts[33]. $AgNO_3$
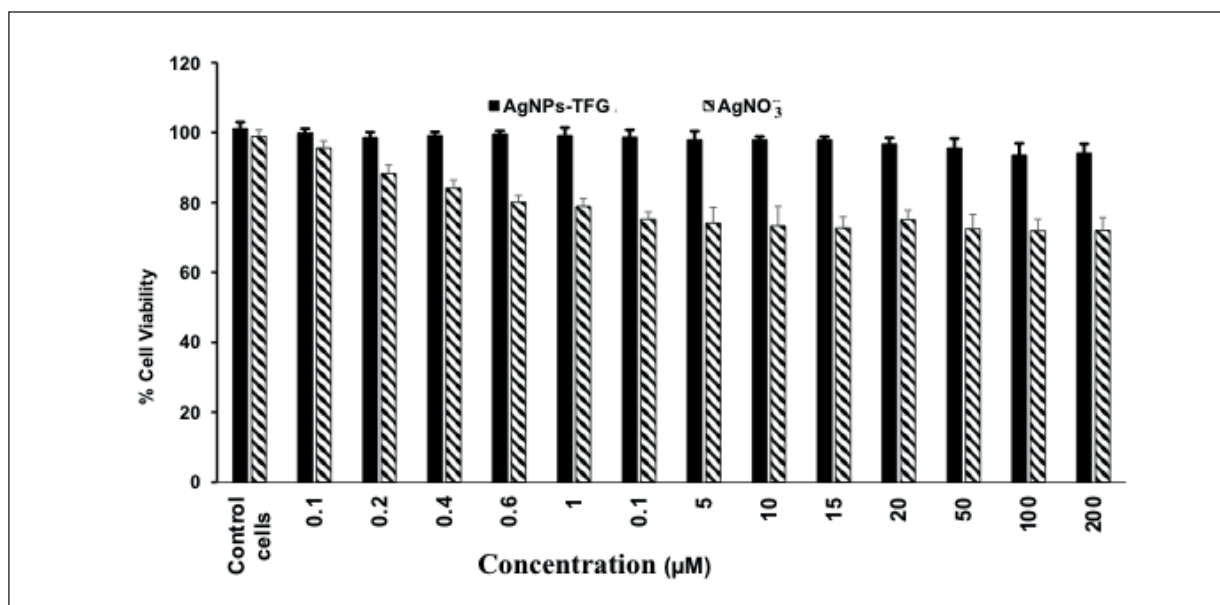

Figure 4. Effects of 0.1-200 *μM* $AgNO_3$ and AgNPs-TFG on the percent viability of MCF-7 cells. Cells were incubated with $AgNO_3$ or AgNPs-TFG for 24 h, and cytotoxicity was examined using CytoTox-Glo Cytotoxicity Assays.
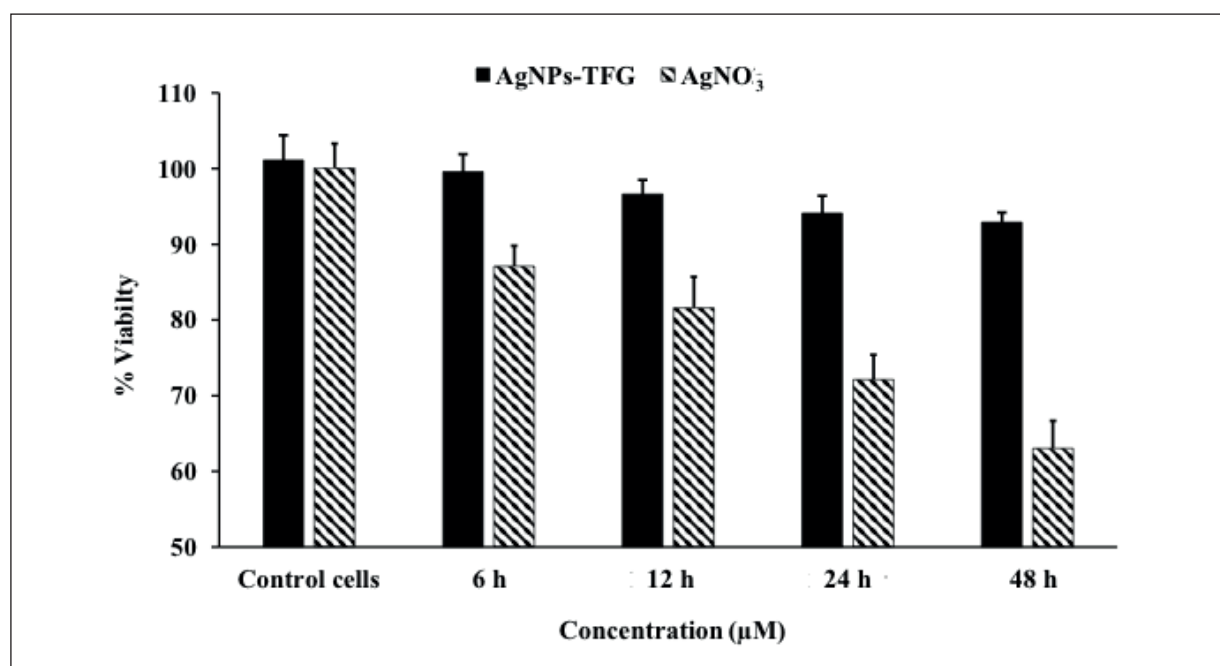
Figure 5. Effects of AgNPs-TFG and AgNO$_3$ on the proliferation of MCF-7 cells. Cell viability was determined in the presence of 200 μM AgNPs-TFG or AgNO$_3$ at 6, 12, 24, or 48 h.

has also been shown to be somewhat cytotoxic to U937 human leukemic monocyte lymphoma cells[34], and another study[35] showed that 100 µg/mL AgNO$_3$ significantly reduced the viability of MDA-MB-231 cells. In this study, we used AgNPs-TFG concentrations of 0.1-200 µM, which are considered safe; this concentration only reduced the viability of the cells by 6% owing to the effects of the silver metal. In another study[36], researchers showed that AgNPs-TFG exhibited anticancer effects on A431 skin cancer cells at concentrations of 600 µM, 1.3 mM, and 2.5 mM, as evidenced by reduced cell growth by 50%, with concentration-dependent effects.

Moreover, MCF-7 cells showed slightly reduced cell viability in the presence of 200 µM AgNPs-TFG at 48 h, which may have been caused by the increased concentration of Ag^0. These findings revealed that AgNPs-TFG caused cytotoxicity by releasing Ag^0 inside the cells[37], consistent with the results of Krishnaraj et al[35], who confirmed that AgNO$_3$ and HAuCl$_4$ exhibited cytotoxic activity against MDA-MB-231 human breast cancer cells.

Further, AgNPs-TFG stimulated the cells and reduced the level *TNF-α* mRNA. Thus, these findings demonstrated that AgNPsTFG decreased TNF-α mRNA and protein expression in MCF-7 cells. As

a result, AgNP-TFG pretreatment may be a feasible therapeutic strategy for breast cancer. The silver ions contained in the prepared AgNPs-TFG caused increased intracellular Ag^0 release, which was responsible for the inhibitory effects of AgNPs-TFG on MCF-7 cells at higher concentrations, in addition to the reduction in TNF-α expression[37]. Moreover, we found that AgNPs-TFG significantly downregulated TNF-α mRNA, consistent with the findings of previous studies[38,39], and suggested that AgNPs-TFG could be used to target various TNF-α-related biological processes, including immune homeostasis, inflammation, apoptosis, proliferation, and tumor invasion.

Conclusions

In this study, we synthesized novel, homogeneously dispersed AgNPs-TFG with acceptable size and PDI using a simple and reproducible green reduction technique. The developed AgNPs-TFG affected the proliferation and gene expression profile of MCF-7 cells, a model of breast cancer. Thus, our novel AgNPs-TFG – inhibiting TNF-α expression – may represent a new affordable approach for anticancer therapy and for the treatment of other inflammation-related illnesses. Further studies are needed to investigate the biocompatibility of Ag-
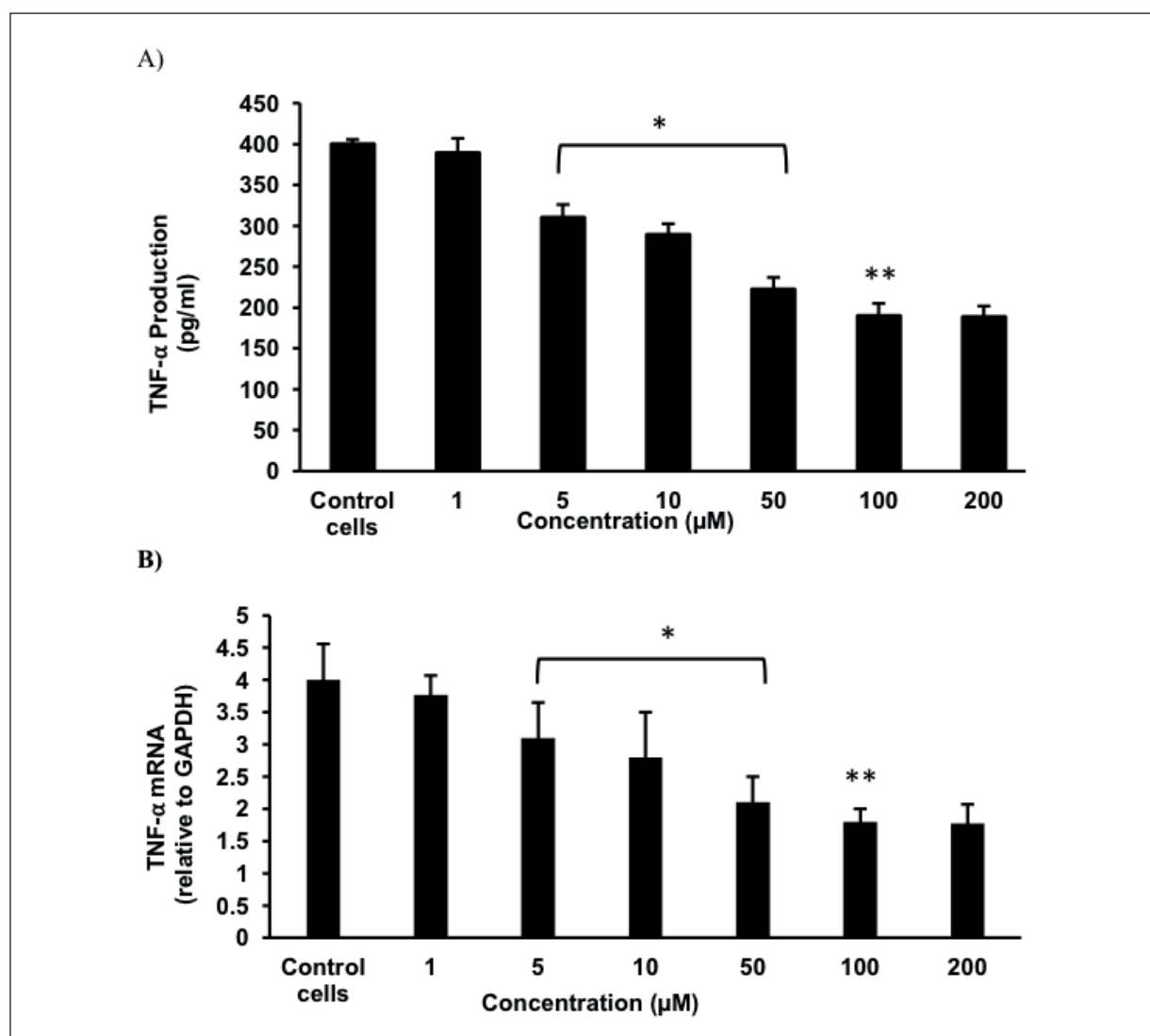
5536

Figure 6. TNF-α mRNA and protein expression. **A**, Effects of AgNPs-TFG on *TNF-α* mRNA levels, as determined by quantitative real-time PCR. **B**, Effects of AgNPs-TFG on TNF-*α* protein production in MCF-7 cells as determined by sandwich ELISA. Results are representative data (means ± standard errors of the means) from triplicate experiments; data without a common letter differ, *$p \leq 0.05$, **$p \leq 0.01$, ***$p \leq 0.001$.

NPs-TFG in human blood, in addition to the pharmacokinetic and pharmacodynamic parameters of the developed AgNPs-TFG. Moreover, additional trials should be conducted to assess the effects of AgNP-TFG formulations as potential treatment modalities in various types of cancer.

Availability of Data and Materials

Not applicable.

Research on Human Participants

No investigation was conducted on human participants in this study.

Conflicts of Interest

The authors declare no conflict of interest.

References

1) Paciotti GF, Kingston DGI, Tamarkin L. Colloidal gold nanoparticles: A novel nanoparticle platform for developing multifunctional tumor-targeted drug delivery vectors. Drug Devt Res 2006; 67: 47-54.

2) Visaria RK, Griffin RJ, Williams BW, Ebbini ES, Paciotti GF, Song CW, Bischof JC. Enhancement of tumor thermal therapy using gold nanoparticle-assisted tumor necrosis factor-alpha delivery. Mol Cancer Ther 2006; 5: 1014-1020.

3) Varghese R, Almalki MA, Ilavenil S, Rebecca J, Choi KC. Silver nanoparticles synthesized using the seed extract of Trigonella foenum-graecum L. and their antimicrobial mechanism and anticancer properties. Saudi J Biol Sci 2019; 26: 148-154.

4) Parveen K, Banse V, Ledwani L. Green synthesis of nanoparticles: Their advantages and disadvantages. AIP conference 2016; 1724: 020048.

5) Tsai DH, Elzey S, DelRio FW, Keene AM, Tyner KM, Clogston JD, MacCuspie RI, Guha S, Zachariah MR, Hackley VA. Tumor necrosis factor interaction with gold nanoparticles. Nanoscale 2012; 4: 3208-3217.

6) Swardfager W, Lanctôt K, Rothenburg L, Wong A, Cappell J, Herrmann N. A meta-analysis of cytokines in Alzheimer's disease. Biol Psychiatry 2010; 68: 930-941.

7) Locksley RM, Killeen N, Lenardo MJ. The TNF and TNF receptor superfamilies: Integrating mammalian biology. Cell 2001; 104: 487-501.

8) Zhou XL, Fan W, Yang G, Yu MX. The clinical significance of PR, ER, NF- kappa B, and TNF-alpha in breast cancer. Dis Markers 2014; 2014: 494581.

9) Perrot-Applanat M, Vacher S, Toullec A, Pelaez I, Velasco G, Cormier F, Saad HE, Lidereau R, Baud V, Bieche I. Similar NF-kappaB gene signatures in TNF-alpha treated human endothelial cells and breast tumor biopsies. PLoS One 2011; 6: e21589.

10) Fehaid A, Taniguchi A. Silver nanoparticles reduce the apoptosis induced by tumor necrosis factor-alpha. Sci Technol Adv Mater 2018; 19: 526-534.

11) Abdellatif AA, Rasheed Z, Alhowail AH, Alqasoumi A, Alsharidah M, Khan RA, Aljohani AS, Aldubayan MA, Faisal W. Silver citrate nanoparticles inhibit PMA-induced TNFalpha expression via deactivation of NF-Kappab activity in human cancer cell-lines, MCF-7. Int J Nanomed 2020; 15: 8479-8493.

12) Abdellatif AAH, Alsharidah M, Al Rugaie O, Tawfeek HM, Tolba NS. Silver Nanoparticle-Coated ethyl cellulose inhibits tumor necrosis factor-alpha of breast cancer cells. Drug Des Devel Ther 2021; 15: 2035-2046.

13) Abdellatif AA, Tawfeek HM. Transfersomal nanoparticles for enhanced transdermal delivery of clindamycin. AAPS PharmSciTech 2016; 17: 1067-1074.

14) Abdellatif AAH, Abou-Taleb HA, Abd El Ghany AA, Lutz I, Bouazzaoui A. Targeting of somatostatin receptors expressed in blood cells using quantum dots coated with vapreotide. Saudi Pharm J 2018; 26: 1162-1169.

15) Abdellatif AAH, Alturki HNH, Tawfeek HM. Different cellulosic polymers for synthesizing silver nanoparticles with antioxidant and antibacterial activities. Sci Rep 2021; 11: 84.

16) Tawfeek HM, Abdellatif AAH, Abdel-Aleem JA, Hassan YA, Fathalla D. Transfersomal gel nanocarriers for enhancement the permeation of lornoxicam. J Drug Deliv Sci Technol 2020; 5: 1015406.

17) Rahman A, Kumar S, Bafana A, Dahoumane SA, Jeffryes C. Biosynthetic conversion of Ag(+) to highly stable Ag(0) nanoparticles by wild type and cell wall deficient strains of Chlamydomonas reinhardtii. Molecules 2018; 24: 98.

18) Fortunati E, Latterini L, Rinaldi S, Kenny JM, Armentano I. PLGA/Ag nanocomposites: In vitro degradation study and silver ion release. J Mater Sci Mater Med 2011; 22: 2735-2744.

19) Rasheed Z, Rasheed N, Al-Shaya O. Epigallocatechin-3-O-gallate modulates global microRNA expression in interleukin-1beta-stimulated human osteoarthritis chondrocytes: Potential role of EGCG on negative co-regulation of microRNA-140-3p and ADAMTS5. Eur J Nutr 2018; 57: 917-928.

20) Pfaffl MW. A new mathematical model for relative quantification in real-time RT-PCR. Nucleic Acids Res 2001; 29: e45.

21) Pereira-Lachataignerais J, Pons R, Panizza P, Courbin L, Rouch J, Lopez O. Study and formation of vesicle systems with low polydispersity index by ultrasound method. Chem Phys Lipids 2006; 140: 88-97.

22) Moraes CM, De Paula E, Rosa AH, Fraceto LF. Physicochemical stability of poly(lactide-co-glycolide) nanocapsules containing the local anesthetic bupivacaine. J Braz Chem Soc 2010; 21: 995-1000.

23) Liu H, Wang D, Song Z, Shang S. Preparation of silver nanoparticles on cellulose nanocrystals and the application in electrochemical detection of DNA hybridization. Cellulose 2010; 18: 67-74

24) Duarte AR, Gordillo MD, Cardoso MM, Simplicio AL, Duarte CM. Preparation of ethyl cellulose/methyl cellulose blends by supercritical antisolvent precipitation. Int J Pharm 2006; 311: 50-54.

25) Raut NS, Somvanshi S, Jumde AB, Khandelwal HM, Umekar MJ, Kotagale NR. Ethyl cellulose and hydroxypropyl methyl cellulose buoyant microspheres of metoprolol succinate: Influence of pH modifiers. Int J Pharm Investig 2013; 3: 163-170.

26) Greenwood R, Kendall K. Selection of suitable dispersants for aqueous suspensions of zirconia and titania powders using acoustophoresis. J Eur Ceramic Soc 1999; 19: 479-488.

27) Kaufman ED, Belyea J, Johnson MC, Nicholson ZM, Ricks JL, Shah PK, Bayless M, Pettersson T, Feldotö Z, Blomberg E, Claesson P. Kaufman ED, Belyea J, Johnson MC, Nicholson ZM, Ricks JL, Shah PK, Bayless M, Pettersson T, Feldotö Z, Blomberg E, Claesson P. Probing protein adsorption onto mercaptoundecanoic acid stabilized gold nanoparticles and surfaces by quartz crystal

microbalance and zeta-potential measurements. Langmuir 2007; 23: 6053-6062

28) He J, Kunitake T, Nakao A. Facile in situ synthesis of noble metal nanoparticles in porous cellulose fibers. Chem Mater 2003; 15: 4401-4406.

29) Liu J, Kershaw WC, Klaassen CD. The protective effect of metallothionein on the toxicity of various metals in rat primary hepatocyte culture. Toxicol Appl Pharmacol 1991; 107: 27-34.

30) Hussain S, Anner RM, Anner BM. Cysteine protects Na, K-ATPase and isolated human lymphocytes from silver toxicity. Biochem Biophys Res Commun 1992; 189: 1444-1449.

31) Teepe RG, Koebrugge EJ, Löwik CW, Petit PL, Bosboom RW, Twiss IM, Boxma H, Vermeer BJ, Ponec M. Cytotoxic effects of topical antimicrobial and antiseptic agents on human keratinocytes in vitro. J Trauma 1993; 35: 8-19.

32) Kaplan A, Akalin Ciftci G, Kutlu HM. The apoptotic and genomic studies on A549 cell line induced by silver nitrate. Tumour Biol 2017; 39: 1010428317695033.

33) Muller G, Kramer A. Biocompatibility index of antiseptic agents by parallel assessment of antimicrobial activity and cellular cytotoxicity. J Antimicrob Chemother 2008; 61: 1281-1287.

34) Kaba SI, Egorova EM. In vitro studies of the toxic effects of silver nanoparticles on HeLa and U937 cells. Nanotechnol Sci Appl 2015; 8: 19-29.

35) Krishnaraj C, Muthukumaran P, Ramachandran R, Balakumaran MD, Kalaichelvan PT. Acalypha indica Linn: Biogenic synthesis of silver and gold nanoparticles and their cytotoxic effects against MDA-MB-231, human breast cancer cells. Biotechnol Rep (Amst) 2014; 4: 42-49.

36) Goyal S, Gupta N, Kumar A, Chatterjee S, Nimesh S. Antibacterial, anticancer and antioxidant potential of silver nanoparticles engineered using Trigonella foenum-graecum seed extract. IET Nanobiotechnol 2018; 12: 526-533.

37) Xu Y, Wang L, Bai R, Zhang T, Chen C. Silver nanoparticles impede phorbol myristate acetate-induced monocyte-macrophage differentiation and autophagy. Nanoscale 2015; 7: 16100-16109.

38) Liu W, Lu X, Shi P, Yang G, Zhou Z, Li W, Mao X, Jiang D, Chen C. TNF-α increases breast cancer stem-like cells through up-regulating TAZ expression via the non-canonical NF-κB pathway. Sci Rep 2020; 10: 1.

39) Josephs SF, Ichim TE, Prince SM, Kesari S, Marincola FM, Escobedo AR, Jafri A. Unleashing endogenous TNF-alpha as a cancer immunotherapeutic. J Translat Med 2018; 16: 1-8.